Stripes, pseudogaps, and Van Hove nesting in the three-band *t-J* model

R. S. Markiewicz
Physics Department and Barnett Institute, Northeastern University, Boston, Massachusetts 02115
(Received 30 January 1997; revised manuscript received 7 April 1997)

Slave-boson calculations have been carried out in the three-band *t-J* model for the high-T_c cuprates, with the inclusion of coupling to oxygen breathing-mode phonons. Phonon-induced Van Hove nesting leads to a phase separation between a hole-doped domain and a (magnetic) domain near half filling, with long-range Coulomb forces limiting the separation to a nanoscopic scale. Strong correlation effects pin the Fermi level *close to*, but not precisely at the Van Hove singularity (VHS), which can enhance the tendency to phase separation. The resulting dispersions have been calculated, both in the uniform phases and in the phase separated regime. In the latter case, distinctly different dispersions are found for large, random domains and for regular (static) striped arrays, and a hypothetical form is presented for *dynamic* striped arrays. The doping dependence of the latter is found to provide an excellent description of photoemission and thermodynamic experiments on pseudogap formation in underdoped cuprates. In particular, the multiplicity of observed gaps is explained as a combination of flux phase plus charge-density-wave (CDW) gaps along with a superconducting gap. The largest gap is associated with VHS nesting. The apparent smooth evolution of this gap with doping masks a crossover from CDW-like effects near optimal doping to magnetic effects (flux phase) near half filling. A crossover from large Fermi surface to hole pockets with increased underdoping is found. In the weakly overdoped regime, the CDW undergoes a quantum phase transition ($T_{\mathrm{CDW}}\rightarrow 0$), which could be obscured by phase separation. [S0163-1829(97)00638-3]

I. INTRODUCTION

The slave-boson technique has frequently been applied to the study of strong correlation effects in metals.[1,2] In the high-T_c cuprate superconductors, the intense theoretical activity now allows a detailed comparison of slave-boson results with the results of quantum Monte Carlo (QMC) or exact diagonalization calculations. Qualitatively, the comparison is excellent: the latter calculations have confirmed slave-boson predictions[2–6] that (1) correlations preserve a Fermi-liquid-like energy dispersion, but renormalize the bandwidth (''flat bands'');[7] (2) a Mott transition to an insulating phase can only occur at exactly half filling, when the bare Cu-O energy splitting Δ_0 is larger than a critical value Δ_{0c} (compare Refs. 8, 9, and 10). The agreement is semiquantitative: the doping dependence of the chemical potential in the three-band model is nearly the same when calculated by slave boson or by quantum Monte Carlo techniques,[11,12] with a slightly smaller value of Δ_{0c} in the latter (Fig. 36 of Ref. 13).

The usual slave-boson technique does not incorporate the magnetic effects which are important near half filling. This may be phenomenologically remedied by including the lowest-order correction in $t^2/U\sim J$, producing a three-band *t-J* model.[14–17] A finite J leads to a small reduction in Δ_{0c}, thereby improving agreement with QMC calculations. The present paper utilizes the three-band *t-J* model to explore the role of Van Hove singularity (VHS) nesting in the cuprates. It is found that VHS nesting provides a natural explanation for the occurence of striped phases, composed of a magnetic-dominated regime near half filling and a charge-dominated regime near optimal doping. The model is found to give a good description of the observed pseudogap formation in these materials, as well as to explain why the charged stripes are pinned near the VHS.

II. SELF-CONSISTENT EQUATIONS

In a recent survey of the Van Hove scenario,[13] it was pointed out that there are actually two variants of the scenario, a *simple* and a *generalized* scenario. The simple scenario explores the role of a peak in the density of states (DOS) on the normal state and superconducting properties, ignoring any possible role of competing instabilities. In the extended scenario, these competing instabilities—predominantly spin- or charge-density waves—play an essential role, which can lead to the suppression of the superconducting instability.

Prior slave-boson calculations had shown that correlation effects (a large on-site Coulomb repulsion, U) tend to pin the Fermi level near the VHS over an extended doping range,[4,6,18] and this has since been confirmed by a number of different techniques.[19–24] It was suggested that nesting of the VHS's would lead to density-wave instabilities which could successfully compete with superconductivity. This was modeled[25] in a one-band tight-binding model, where the pinning was approximated by adjusting the Fermi surface curvature such that the Fermi level was exactly at the VHS for all dopings. The resulting density wave-superconducting phase diagram is in good agreement with the experimentally observed pseudogap transition vs doping.[26]

Clearly, such a model is oversimplified. Strong correlation effects tend to suppress electron-phonon coupling near half filling, suggesting that the density wave must cross over from spin-density-wavelike near half filling to charge-density wavelike near optimal doping. Whether such a cross-

 © 1997 The American Physical Society

over could be adequately described in a one-band model was not at all clear.

In the present paper, a self-consistent three-band *t-J* model calculation is presented for this crossover, confirming the main results of the simpler calculation, and suggesting a possible origin of striped phases in these materials. The three-band *t-J* model Hamiltonian is the same as that presented in Ref. 17, with the addition of a term due to the formation of a charge-density wave (CDW) of breathing mode symmetry. No spin-dependent terms are included, so the present model does not describe either the Néel or the superconducting phases. Both the CDW and the magnetic flux phase, if present, break the symmetry of the even and odd Cu sites in a given layer, giving rise to a doubling of the unit cell area. In a basis set consisting of symmetric and antisymmetric combinations of the atoms on the two sublattices, the Hamiltonian matrix becomes

$$\begin{pmatrix} \Delta_+ & -2its_x & -2its_y & -i\Delta_m & -2tc_x\delta_b & -2tc_y\delta_b \\ 2its_x & 0 & u_0 s_x s_y & -2its_x\delta_a & 0 & 0 \\ 2its_y & u_0 s_x s_y & 0 & -2its_y\delta_a & 0 & 0 \\ i\Delta_m & 2its_x\delta_a & 2its_y\delta_a & \Delta_- & 2tc_x & 2tc_y \\ -2tc_x\delta_b & 0 & 0 & 2tc_x & 0 & u_0 c_x c_y \\ -2tc_y\delta_b & 0 & 0 & 2tc_y & u_0 c_x c_y & 0 \end{pmatrix}, \tag{1}$$

where $\Delta_\pm = \Delta \pm \Delta_p$. In this matrix, the band parameters are Δ, the splitting between the Cu and O energy levels, $t_{\mathrm{CuO}} = t(1 \pm \delta)$, the Cu-O hopping parameter, t_{OO}, the O-O hopping parameter, and Δ_1 a parameter associated with Cu-Cu exchange. In addition, $c_i = \cos(k_i a/2)$, $s_i = \sin(k_i a/2)$, $i = x,y$, and $u_0 = -4t_{\mathrm{OO}}$.

δ is the asymmetry of the Cu-O hopping introduced by the CDW distortion; for a breathing mode, all four Cu-O bonds of one Cu are long $[t_{\mathrm{CuO}} = t(1-\delta)]$, while all four bonds for the other Cu are short. There are two possible values for δ: let

$$\delta_k = \begin{cases} \delta_0 + \delta_1, & \text{if } |E_k' - E_F| \leqslant \hbar\omega_0; \\ \delta_0, & \text{otherwise,} \end{cases} \tag{2}$$

with ω_0 a phonon cutoff frequency and E_k' the quasiparticle energy in the absence of a CDW. The use of E_k' in Eq. (2) is a weak coupling approximation; it will be seen to lead to a slightly erroneous dispersion, in that the resulting gap is not exactly centered at E_F. In the Hamiltonian matrix, Eq. (1), the δ_i $i = a,b$ should be replaced by the appropriate δ_k, which may be different for the symmetric and antisymmetric Cu's.

At the mean-field level, magnetic exchange leads to an effective Cu-Cu hopping, of magnitude

$$\Delta_{ij} \equiv J \sum_\sigma \langle d_{i\sigma} d_{j\sigma}^\dagger \rangle = \Delta_1 e^{i\theta_{ij}}, \tag{3}$$

with i and j labeling adjacent Cu sites. A number of different magnetic phases are possible, depending on the choice of phase. Here only two magnetic phases are considered, the paramagnetic ($\theta_{ij} = 0$) and the flux ($\theta_{ij} = \pm\pi/4$) (Ref. 27) phases. The paramagnetic phase is usually called the uniform phase, but here ''uniform'' will be used in a different way, to denote the absence of a phase separation. In the flux phase, the $\pm$ sign is chosen so that the net phase change around any plaquette is $\pm\pi$. For the paramagnetic phase, $\Delta_p = -2\Delta_1(\overline{c_x} + \overline{c_y})$, $\Delta_m = 0$, with $\overline{c_i} = \cos k_i a$, $i = x,y$. For the flux phase, $\Delta_p = -\sqrt{2}\Delta_1(\overline{c_x} + \overline{c_y})$ and $\Delta_m = -\sqrt{2}\Delta_1(\overline{c_x} - \overline{c_y})$.

If the unrenormalized values of Δ and t are Δ_0 and t_0, respectively, then setting $r_0 = t/t_0$, the equations of self-consistency become

$$r_0^2 = \frac{1}{2}\left[1 - \frac{1}{N_s}\sum_k u_k^2 f_h(E_k)\right], \tag{4}$$

$$\Delta_0 - \Delta = \frac{1}{2r_0^2 N_s}\sum_k u_k^2 f_h(E_k)(E_k - \widetilde{\Delta}), \tag{5}$$

and

$$\Delta_1 = \frac{J}{2N_s}\sum_k u_k^2 f_h(E_k)\gamma_{\vec{k}}, \tag{6}$$

where N_s is the number of unit cells E_k is the eigenvalue of H, $f_h(E_k)$ is the Fermi function, u_k is the amplitude of the wave function on Cu, and $\widetilde{\Delta} = \Delta + 2\Delta_1\gamma_{\vec{k}}$. The function $\gamma_{\vec{k}} = \overline{c_x} + \overline{c_y}$ $(\sqrt{\overline{c_x^2} + \overline{c_y^2}})$ in the paramagnetic (flux) phase. As written, Eqs. (4) and (5) are valid for a hole picture, so $f_h(E_k) = 1$ for $E_k > E_F$, and $= 0$ otherwise (assuming $T = 0$). The Fermi energy is determined from

$$\frac{1}{N_s}\sum_k f_h(E_k) = 1 + x. \tag{7}$$

For the CDW, the additional self-consistent equations are[28]

$$\delta_0 = \frac{-V_{\mathrm{ep}}}{2tN_s}\sum_k{}'' f_h(E_k) u_{1k}^*(v_{2x}c_x + v_{2y}c_y), \tag{8}$$

$$\delta_1 = \frac{-V_{\rm ep}}{2tN_s}\sum_k{}'' f_h(E_k) u_{1k}^* (v_{2x}c_x + v_{2y}c_y), \tag{9}$$

where $V_{\rm ep}$ is the phonon-induced effective electron-electron interaction energy and the double prime on the first sum means that both $|E_k' - E_F| \leqslant \hbar\omega_0$ and $|E'_{|\vec{k}+\vec{Q}|} - E_F| \leqslant \hbar\omega_0$, with $\vec{Q} = (\pi/a, \pi/a)$. Also, u_1 is the wave function amplitude for one (e.g., the symmetric) Cu, and v_{2x}, v_{2y} are the corresponding amplitudes for the (antisymmetric) oxygens.

In the present paper, the parameters are taken as $\Delta_0 = 6$ eV, $t_0 = 1.3$ eV, $t_{\rm OO} = -0.45$ eV, $J = 0.13$ eV, and $\hbar\omega_0 = 50$ meV.[13] The free energy is ($f_e = 1 - f_h$)

$$F = F_0 + \sum_k f_e(E_k) E_k, \tag{10}$$

$$F_0 = N_s \left[(\Delta_0 - \Delta)(1 + 2r_0^2) + \frac{2\Delta_1^2}{J} + \frac{t^2 \delta_0 \delta_1}{V_{\rm ep}} \right]. \tag{11}$$

III. PHASE SEPARATION

A. Search for phase separation

There is considerable experimental evidence for phase separation in the cuprates, which has been presented in a number of conferences[29] and reviews.[30,31,13] For the hole-doped cuprates, the phase separation is believed to be between a hole-doped phase and an antiferromagnetic insulator (AFI) phase close to half filling. The experimental evidence for this latter case falls into two categories, depending on whether the dopant ions are mobile or not. Thus, in $La_2CuO_{4+\delta}$, the doping is provided by interstitial oxygens[32] which are mobile below room temperature. When the holes bunch up, the interstitial O's follow, leading to a macroscopic phase separation between an undoped AFI and an optimally doped high-T_c superconductor. In other cuprates, the dopant ions are immobile, and the phase separation is restricted to a nanoscopic scale due to Coulomb repulsion between holes. Tranquada and co-workers[33,34] have demonstrated that in $La_{2-x-y}Nd_ySr_xCuO_4$, when $x \sim 1/8$, commensurability effects pin the domains, allowing a clear observation of alternating charged and magnetic stripes. They suggest that similar stripes exist in other cuprates, but as dynamic fluctuations.

There have been a number of theoretical suggestions that phase separation arises in a doped Mott insulator, some[35,36] prior to the discovery of high-T_c superconductivity, and others[37,38,4] in the specific context of the cuprates. However, detailed calculations have generally found that phase separation is either absent (in the pure Hubbard model[39,40]) or is present only for unphysically large choices of parameters, such as J (in the t-J model),[40] or the nearest neighbor Coulomb energy V (in the three-band extended Hubbard model).[41] Some recent calculations of the t-J model have suggested that phase separation persists to lower values of J,[42,43] but these results remain controversial.

The present calculations show no evidence of phase separation in the absence of electron-phonon coupling. Figure 1 shows the doping dependence of the free energy for both the paramagnetic (solid line) and flux (dashed line) phases, when $V_{\rm ep} = 0$.[17] The cusp at half filling is indicative of the transition to a charge-transfer insulating state at half filling (discontinuity of the chemical potential). At half filling, the flux phase is more stable than the paramagnetic phase. There is a crossover to the paramagnetic phase near $x = -0.09$ for electron doping, or $x = 0.38$ for hole doping. In the present calculation, these appear to be first-order transitions, but if the flux per plaquette is not restricted to the values zero and π [the phase θ_{ij} in Eq. (3) is allowed to vary continuously[15,16]], then there is a smooth crossover from the flux to the paramagnetic phase, without a discontinuous jump (see Ref. 44).

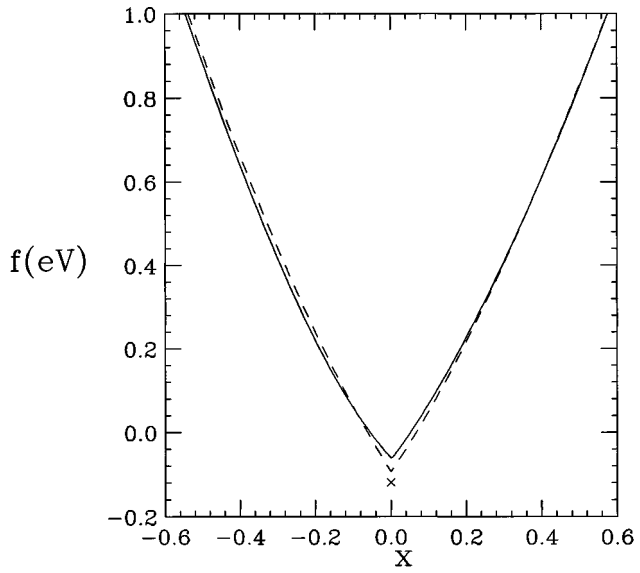

FIG. 1. Comparison of free energies in the paramagnetic (solid line) and flux (dashed line) phases. To accentuate the curvature in f, a term linear in x has been subtracted from all curves. The t-J model result at half filling is indicated by a $\times$.

The present slave-boson calculation underestimates the free energy at half filling, due to neglect of Néel order. Since $t \to 0$ at half filling, the oxygen bands decouple from the problem, and the free energy should be identical to that found in the one-band t-J model, and hence in the Hubbard model. This energy is known to be $E_H = -0.669\,34J$.[43,45] As denoted by the $\times$ in Fig. 1, this is $\sim 50\%$ lower than the flux phase result. (This estimate neglects a term $-n_{\rm Cu}J/2$, which is common to all the magnetic phases and changes only weakly with doping. Here $n_{\rm Cu}$ is the average hole density on the Cu.) Since the Néel transition decreases rapidly with doping, the free energy curve should cross over from the $\times$ to the dashed line at a fairly low doping value. While there are other factors which can further lower the free energy near half filling, such as a spin-Peierls phase,[46,47] it does not appear that such effects will introduce a tendency toward phase separation.

Instead, one might invoke a *lever rule for phase separation*: a relatively small perturbation can drive the system to phase separate, if it is applied with an appropriate *lever arm*. Since a cusp is already present at half filling, it will be much more effective *to introduce a second free energy dip away from half filling*.

B. VHS nesting induced phase separation

Figure 2 compares the free energy $f = F/N_s$ for the paramagnetic phase for two values of $V_{\rm ep} = 0$ or 1 eV to that of

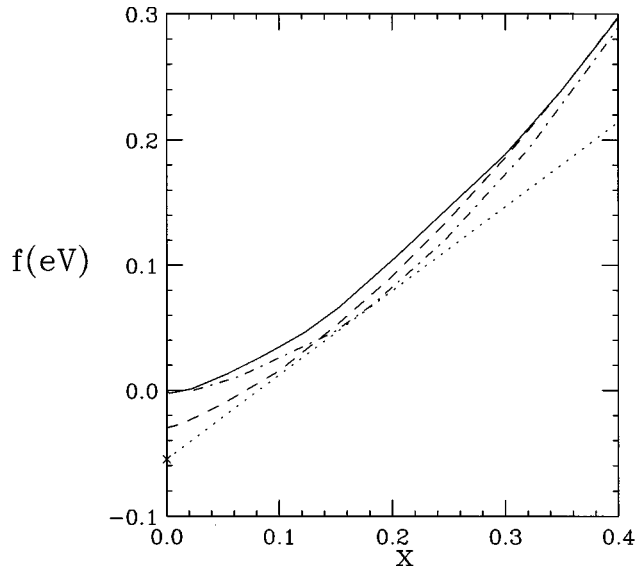

FIG. 2. Free energy $f=F/N_s$ in the paramagnetic phase as a function of hole doping x, for electron-phonon coupling $V_{ep}=0$ (solid line) or 1 eV (dot-dashed line), compared to the flux phase (dashed line). A term linear in x has been subtracted from all curves. The t-J model result at half filling is indicated by a $\times$; dotted line is the tangent construction for two-phase coexistence.

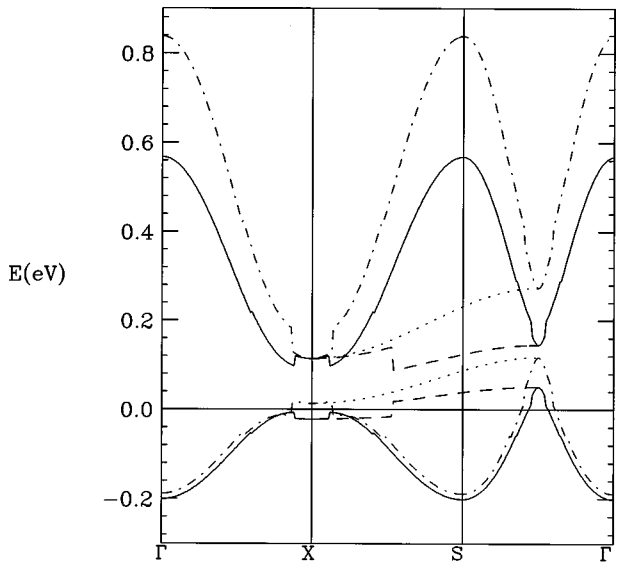

FIG. 3. Energy dispersion for the paramagnetic phase, for $V_{ep}=1$ eV, for $x=0.15$ (solid lines) or 0.32 (dot-dashed lines). The dashed and dotted lines are the corresponding dispersions from X to $\overline{S}=S/2$.

the flux phase. In the paramagnetic phase, a charge-density wave (CDW) lowers the free energy by opening a gap at the VHS, lowering the electronic energy of occupied states. (The nature of the resulting CDW state is discussed further in the following section.) Since the VHS degeneracy is already split in the flux phase (Fig. 7 below), no additional energy lowering is possible, and the CDW is not compatible with the flux phase. From Fig. 2, it can be seen that the free energy lowering due to the CDW has a strong x dependence: the free energy lowering vanishes as $x\rightarrow 0$ and is absent for electron doping. It also vanishes for too large hole doping. This result is due to VHS nesting: the strongest CDW effects occur when the Fermi level is close to the VHS.

These results confirm and quantify the prediction[4] that electron-phonon coupling near the VHS produces a dip in the free energy, which can generate a phase separation. The curves of free energy for the CDW phase and the flux phase cross at a finite hole doping, x. Since it is not possible for the system to smoothly evolve between the two phases, this indicates a first order phase transition, with a two-phase coexistence regime given by a tangent construction. In Fig. 2, it is assumed that the phase separation starts from the AFI phase at half filling (denoted by $\times$), but depending on the exact dispersion, the free energy minimum may be shifted off of half filling. The metallic phase will tend to be pinned near the VHS, as discussed further in the following section.

Note that the present calculation is perhaps the strongest indication to date that phase separation can arise in the cuprates with a realistic choice of band parameters.

In the following, it will be assumed that there is a phase separation between a flux phase with $x=x_1$ and a CDW phase with $x_c\simeq 0.2$. The precise value of x_c is not important, but it will turn out to make a difference whether the flux phase is at $x_1=0$ or 0^+. Before this phase separation is analyzed, the properties of the uniform phases will be briefly discussed.

IV. RESULTS: UNIFORM PHASES

A. CDW gap

Whereas equations Eqs. (8) and (9) represent a BCS-like calculation of the CDW gap,[28] the nature of the gap is very different from that found in a superconductor, since the pairing now involves an electron and a hole. From Eq. (2), there are *two gaps* with very different properties. The term δ_0 produces a uniform gap throughout the Brillouin zone. This gap is *not* tied to the Fermi level, but has its own dispersion throughout the zone. However, it *is* tied to the VHS, and always splits the VHS DOS peak into two components. On the other hand, the gap associated with δ_1 is localized near the Fermi level, but need not split the VHS degeneracy.

In the cuprates, it will be shown that the gaps near the VHS's tend to change the large Fermi surface into pockets near the $(\pi/2,\pi/2)$ points. Since the δ_1 gap only acts to enhance the δ_0 gap, the Fermi surface near these pockets remains ungapped, and hence available for, e.g., superconducting pairing.

These features are illustrated in Fig. 3, for two different dopings with $V_{ep}=1$ eV. For both dopings, δ_0 leads to a similar splitting of the VHS degeneracy, but the δ_1-associated gap is very different. For $x=0.32$, the Fermi level is more than $\hbar\omega_0$ below the VHS, so there is a larger gap away from the VHS. For $x=0.15$, the VHS is now within $\hbar\omega_0$ of the Fermi level, but now for both of the bands coupled by nesting [i.e., in Eq. (1), $\delta_a=\delta_b=\delta_0+\delta_1$], so there are actually two δ_1 type gaps near the VHS. Note that the gap associated with δ_1 is not exactly centered at E_F, and indeed has some dispersion of its own. This is due to the weak coupling Eq. (2), which measures the gap from the bands *in the absence of electron-phonon coupling*.

When Eq. (1) is Fourier transformed back to real space (and deconvolved from a symmetric/antisymmetric basis to an atomic basis), the term $\delta_a+\delta_b$ is found to correspond to a uniform breathing-mode distortion, while $\delta_a-\delta_b$ produces

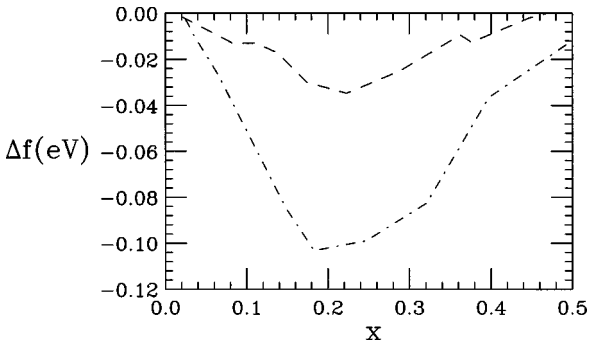

FIG. 4. Free energy difference $\Delta f = f(V_{ep}) - f(0)$ for the paramagnetic phase with $V_{ep} = 0.6$ eV (dashed line) and 1.0 eV (dot-dashed line).

an additional modulation with periodicity $\sim k_F^{-1}$, where $\vec{k}_F$ is the wave number at the enhanced gap. This can be understood on the basis of simple hole counting: The uniform breathing-mode distortion causes a doubling of the unit cell area. This can only produce a gap at exactly half filling (corresponding to a filled band in the supercell). To produce a gap at $x \neq 0$ requires a large superlattice, as would be produced by a commensurate value of $\vec{k}_F$.

These results clarify an issue that had been raised earlier.[48] Whereas CDW effects have traditionally been associated with Fermi surface nesting, it was pointed out that polaronic band narrowing effects can be pinned to the VHS, and not the Fermi level, and hence can explain the observation of *extended* VHS's.[49] Here we see that there are three related effects. The δ_0 gap is associated with the polaronic effects tied to the VHS, and will be seen to describe the photoemission observations of extended VHS's. In addition, there is an extra gap associated with δ_1, when the quasiparticle energy is close to the Fermi level. Finally, this latter gap has a nesting enhancement when two pieces of Fermi surface are separated by the nesting vector [here, $Q = (\pi/a, \pi/a)$]. From Eq. (9), only in the latter case does the gap contribute to the self-consistent equation for δ_1.

B. VHS pinning

Figure 2 shows a crossover in free energy between the flux phase near half filling and the CDW phase near the VHS, which leads to a regime of phase separation. In this subsection, the doping dependence of the CDW phase is discussed in the absence of phase separation. Since the CDW couples to the electronic subsystem via modulation of the hopping parameter, the free energy lowering due to the CDW vanishes as $x \to 0$, where correlation effects drive $t \to 0$. When the hole doping gets too large, the Fermi level moves beyond the VHS, and the stabilization energy also vanishes. Hence, the strongest CDW effects occur when the Fermi level is close to the VHS (VHS nesting). Note that, since the *shape* of the Fermi surface is doping dependent, the VHS remains pinned close to the Fermi level over an extended doping range. Nevertheless, the free energy lowering has a well defined maximum. This is better seen in Fig. 4, which plots the difference in free energy between the calculations for finite V_{ep} and those with $V_{ep} = 0$. This free energy

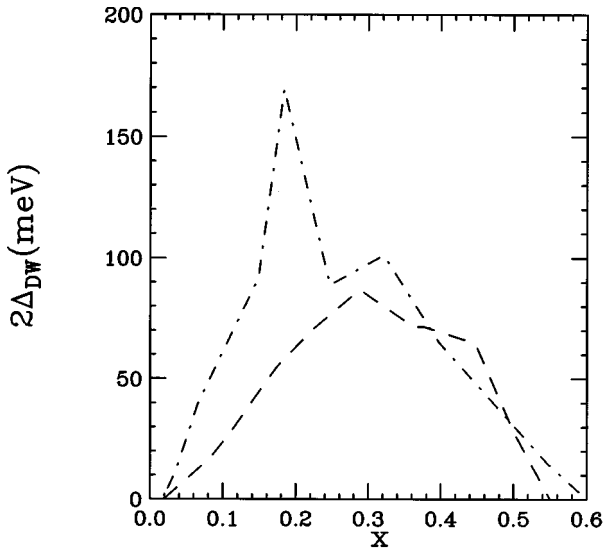

FIG. 5. CDW gap $2\Delta_{DW}$ plotted vs doping in the paramagnetic phase for $V_{ep} = 0.6$ eV (dashed line), or 1 eV (dot-dashed line).

lowering is approximately quadratic in V_{ep}, with a doping dependence which roughly follows the magnitude of the CDW gap, Δ_{DW}, Fig. 5.

The CDW formation also greatly enhances the pinning of the Fermi level to the VHS. Figure 6 plots the energy difference between the VHS and the Fermi level. In the absence of electron-phonon coupling (solid line), the Fermi level crosses the VHS twice, at $x = 0$ and $x = \tilde{x}_c$, and correlation effects pin the Fermi level close to the VHS for $0 \leq x \leq \tilde{x}_c$. However, for the large assumed value $t_{OO} = -0.45$ eV, $\tilde{x}_c$ is small, leading to pinning in a narrow range of doping only. In the presence of a CDW, the energy bands split near the X point of the Brillouin zone, Fig. 7, with each X-point band edge forming a separate VHS DOS peak. The Fermi level is now even further from the average position of the VHS, taken as the middle of the X-point gap. However, the *lower*

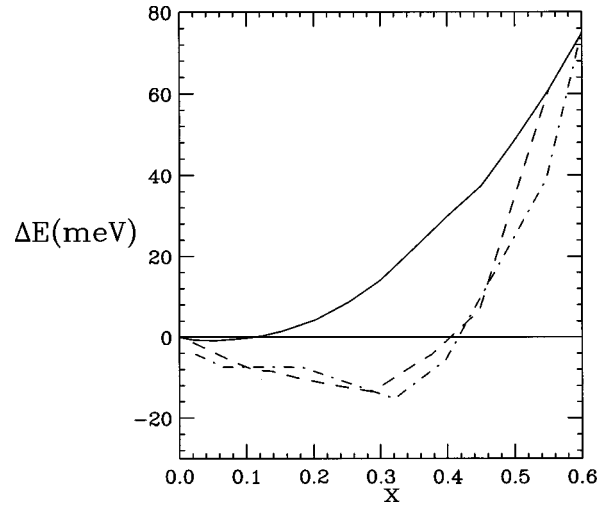

FIG. 6. Energy separation between the VHS and the Fermi level $\Delta E = E_{VHS} - E_F$, in the paramagnetic phase for $V_{ep} = 0$ (solid line), 0.6 eV (dashed lines), or 1 eV (dot-dashed lines). For $V_{ep} \neq 0$, the VHS is split; the present lines refer to the lower VHS's. For the $V_{ep} = 1$ eV data, the extra splitting due to δ_1 is neglected.

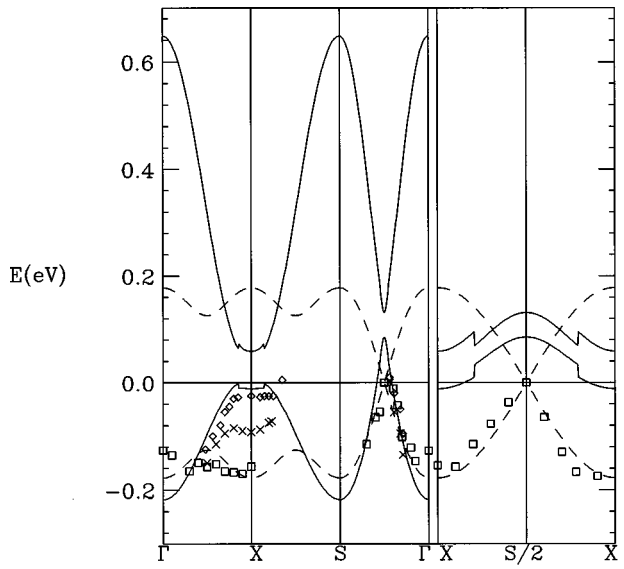

FIG. 7. Energy dispersion for the flux phase at half filling $x_1=0^+$ (dashed line) and the paramagnetic phase at $x=0.22$, $V_{ep}=0.6$ eV (solid line), close to the minimum of Δf. Data from underdoped Bi-2212 (diamonds and $\times$'s) (Ref. 50) or SCOC (squares) (Ref. 51) are plotted as $E/2$. Special points of the Brillouin zone are $X=(\pi,0)$, $S=(\pi,\pi)$.

VHS peak is found to be pinned about 10–20 meV *below the Fermi level over a wide range of dopings*, Fig. 6. This is in striking agreement with photoemission observations of optimally doped cuprates. Due to this strong pinning effect, it is difficult to define just what doping corresponds to *the* VHS. However, the hole-doped end phase of the phase separation regime will almost certainly be found to be pinned near a VHS.

These electron-phonon effects are found to be absent in the flux phase. This is because the flux phase itself has already taken advantage of VHS nesting to lower its free energy, as can be seen in Fig. 7.

The solid line in Fig. 6 bears a close resemblance to the results of earlier slave-boson calculations which neglected the exchange terms in J, e.g., Fig. 13(d) of Ref. 9. However, the exchange has led to a profound modification of the resulting physics. In the earlier calculations, $E_{\rm VHS}-E_F\rightarrow 0$ at half filling because the bandwidth was itself renormalized to zero. However, the Fermi surface at half filling is clearly far from the VHS, Fig. 14 of Ref. 9. The reason is somewhat subtle: since the VHS is shifted off of half filling by the term $t_{\rm OO}$, and at half filling the holes are completely on the Cu's, how can a term involving oxygen-oxygen hopping modify the dispersion? The problem is that in the usual slave-boson model, there is no direct Cu-Cu type hopping, so the *Cu band would be completely dispersionless in the absence of Cu-O hopping*. Thus, both the bandwidth and $E_{\rm VHS}-E_F$ vanish at half filling, but their ratio remains constant. In light of this, the modifications due to exchange J can be readily understood. Now t still vanishes at half filling, but the bandwidth $\sim 2J$ does not. Thus, now any residual curvature associated with $t_{\rm OO}$ really does become negligible at half filling, and the Fermi surface is determined entirely by J. As will be shown later, Sec. IV C, Eq. (12), this means the Fermi surface is square (i.e., at the VHS) at half filling in the paramagnetic phase, and has small pockets near half filling in the flux phase, Fig. 15.

While there is no evidence for long-range CDW order in the cuprates, there is considerable evidence for short-range lattice disorder, summarized in Ref. 13, Sec. 9.2. While a substantial part of this local order is associated with tilting the CuO_6 octahedra out of the planes, there is also a significant contribution associated with CuO bond stretching.[48] Considerable work will be required to sort out the relative contributions of various phonon modes. For now, the breathing mode CDW is chosen to approximately represent the free energy lowering associated with this short-range order.

C. Insulating regime

At half filling, for $\Delta_0>\Delta_{0c}$, there is an insulating phase with $r_0=0$, but $\Delta_1\neq 0$, with energy dispersion

$$E=\Delta+2\Delta_1\gamma_{\vec{k}}. \tag{12}$$

At this doping, the free energy has a cusp (Fig. 2), so the chemical potential has a discontinuity: Δ in Eq. (12) takes on different values depending on whether $x=0$ is approached from positive or from negative values. These two states have the same free energy, even though their effective Fermi levels differ by the charge-transfer gap. Hence the chemical potential is pinned in the middle of the gap, and photoemission should see a band with finite dispersion, Eq. (12), separated from the chemical potential by half the charge-transfer gap.

Note that this band is only half full, but because of strong correlation effects the remaining states are no longer accessible. This is reminiscent of the upper and lower Hubbard bands, although these are now charge-transfer bands. This splitting of the band is readily done in the flux phase, since the lower and upper halfs of the band are only connected at a few isolated points (diabolical points). However, it creates topological problems for the paramagnetic phase. Since the Fermi surface in the paramagnetic phase is square [at exactly half filling, Eq. (12)], these problems can easily be overcome by opening a gap at the Fermi level—either due to antiferromagnetism or to a period doubling charge-density wave. Note that this strongly suggests that the opening of a correlation gap must be accompanied by some other kind of ordering.

The split-off charge transfer band may have been observed experimentally.[51] Since $t\rightarrow 0$, the dispersion is independent of all hopping parameters (e.g., $t_{\rm OO}$). Hence, in the absence of longer-range exchange terms, the dispersion should be characteristic solely of the type of magnetic order, and should be the same as in the one band t-J model. Thus, it is interesting to note that the dispersion in the paramagnetic phase matches that calculated in the t-J model,[52,53] while the flux phase dispersion matches that found in insulating $Sr_2CuO_2Cl_2$ (SCOC),[51] Fig. 7. This is consistent with the results of Laughlin[54] and Wen and Lee.[55]

The magnitude of the predicted bandwidth can also be estimated. Using the mean-field decoupling, the equilibrium value of Δ_1 in the paramagnetic phase is $4J/\pi^2=0.406J$, which is comparable to that found in Ref. 52, $\Delta_1\simeq 0.55J$. In the flux phase, $\Delta_1=0.479J$, so $f=-2\Delta_1^2/J=-0.459J$, con-

siderably smaller than the one band t-J result, $E_H = -0.669\,34J$. As discussed above, this is presumably due to neglecting the Néel order, and will be addressed in a future publication. Δ_1 monotonically decreases in magnitude as the system is doped away from half filling (in agreement with four-slave-boson calculations[56]).

D. Flux phase and VHS nesting

Within the present model, the flux phase has what is interpreted as a gauge degree of freedom:[27,57,13] the energy does not depend on the individual phases θ_{ij} in Eq. (3), as long as the sum of the phases around a plaquette is π. However, different choices of θ_{ij} lead to *different electronic dispersions*. Since the electronic dispersion is observable (e.g., by photoemission), this cannot be simply a choice of gauge. For instance, the present choice (all phases equal in magnitude to $\pi/4$) leads to an ''extended s-wave'' type gap, with zero gap at the four points equivalent to $(\pi/2,\pi/2)$ and a maximum gap at the $(\pi,0)$-type points; this is equivalent to a VHS nesting gap. Alternatively, concentrating the full phase π on a single bond (with $\theta_{ij}=0$ on the other three bonds) leads to gap zeros at the $(\pi,0)$ points, and maxima at the $(\pi/2,\pi/2)$ points—corresponding to conventional (flat Fermi surface) nesting—see Fig. 32(b),(c) in Ref. 13. Both phases have the same energy, and yet experimentally only the former is observed, Fig. 7.

It is the discreteness of the CuO_2 lattice which breaks the gauge symmetry—e.g., in photoemission, the position of the Γ point is well defined. Similarly, it is presumably a structural distortion (spin-Peierls-like effect) which breaks the energy degeneracy, and locks in a particular distortion pattern. This will be explored further in a future publication.

V. PSEUDOGAPS IN THE UNDERDOPED REGIME

A. The experimental situation

Above, it was shown that the CDW gap is expected to have two components, one tied to the VHS and one to the Fermi surface. In a similar fashion, photoemission studies in underdoped $Bi_2Sr_2CaCu_2O_8$ (Bi-2212) find two gaplike features, one tied to the Fermi level, and the other much larger gap near the VHS. The *small pseudogap* resembles a superconducting gap, with the photoemission intensity collapsing to zero for $|E-E_F| \leq \Delta_{\rm sm}(\vec{k})$; the *large pseudogap* is a shift of a broadened quasiparticle-like peak away from the Fermi level, predominantly near $(\pi,0)$ and $(0,\pi)$. The small pseudogap has a d-wave-like symmetry, with a maximum value of 25 meV near $(\pi,0)$ and a minimum value of ~ 0 near $(\pi/2,\pi/2)$.[58,59] The gap magnitude is nearly independent of doping, but it opens up at the pseudogap temperature—i.e., at the superconducting transition in optimally doped material, but at a higher temperature in underdoped samples. This gap thus has some features of the Fermi surface CDW gap discussed above, but combined with the superconducting gap. This near Fermi surface feature will be analyzed further in the discussion section. Here, I would like to concentrate on the large pseudogap.

In the underdoped regime, the photoemission studies find a peak near the X point, which shifts further below the Fermi level with increasing underdoping,[50] Fig. 7. The Stanford group[50] reports a continuous evolution of this peak with underdoping, approaching a dispersion near half filling similar to that found in the insulating compound SCOC,[51] squares in Fig. 7.

On the other hand, Campuzano[60] proposes a different doping dependence of this feature. He suggests that there are two independent features near $(\pi,0)$ in the Brillouin zone, one a sharp quasiparticle peak which is near the Fermi level at optimal doping, and broadens severely in underdoped samples, and the second a broad peak which is already present at ~ 200 meV below the Fermi level in optimally doped material, and gradually shifts to 300 meV with increased underdoping. The present model suggests an intermediate position: the data can be understood as a dynamic average of the two separated phases represented by the solid and dashed lines in Fig. 7. If the fluctuations are fast compared to the experimental observation technique, the data will give an average dispersion which evolves smoothly with doping. A quasistatic fluctuation, on the other hand, would produce two coexisting peaks, with one peak gradually disappearing as the other peak grows up with underdoping.

Thermodynamic measurements of the pseudogap by Loram *et al.*[61,62] in underdoped $YBa_2Cu_3O_{6+y}$ (YBCO) and LSCO are in good agreement with the Stanford photoemission data.[50] They have measured the DOS from susceptibility and heat capacity measurements and find that a pseudogap appears and grows with successive underdoping. At $y=0.3$ in YBCO, the peak of the gap is at $\Delta_g \simeq 100$ meV, comparable to the larger photoemission gap seen in Bi-2212. The gap can be fit to a d-wave gap—i.e., a logarithmic divergence at $E=E_F+\Delta_g$, as at a VHS, but with the DOS$\rightarrow 0$ at $E \rightarrow E_F$. Presumably, these measurements are seeing a superposition of the two gaps seen in photoemission.

There are also photoemission data on underdoped YBCO,[63,64] but they do not reveal a similar gap opening. Since the effects are rather subtle, additional measurements may be needed.

B. Pseudogaps in the uniform phases

Figure 7 compares the dispersion observed for a series of underdoped samples of $Bi_2Sr_2Ca_{1-x}Dy_xCuO_8$ with the theoretical dispersions from the two equilibrium phases at $x=0^+$ and $x=x_c$. For the present choice of band parameters, the bandwidth is underestimated by about a factor of two, but the theoretical calculations match the overall dispersion in the optimally doped and extremely underdoped limits. Indeed, as far as the large pseudogap is concerned, its doping dependence is fairly well explained by the fact that it evolves into the flux phase at half filling.

Thus, Fig. 8 shows the energy dispersion in a series of uniform (flux or paramagnetic) phases, corresponding to the free energy curves in Fig. 1. As the flux phase is doped away from half filling (perfect nesting), the X-point gap gradually closes. The transition to the paramagnetic phase occurs when the lower VHS gets too close to the Fermi level. Note that the doping dependence already does a good job of reproducing the photoemission data on the large pseudogap (consistent with the results of Preuss *et al.*[65]), but cannot reproduce the small, ~ 25 meV pseudogap. On the other hand, when $V_{\rm ep} \neq 0$, the paramagnetic phase near optimal doping clearly

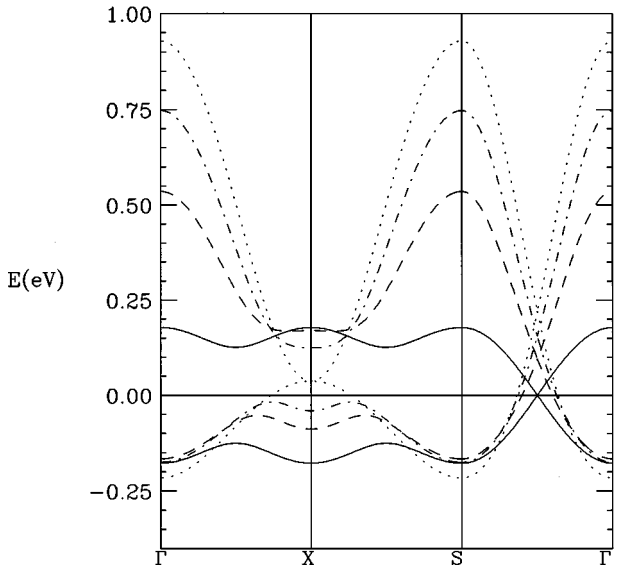

FIG. 8. Energy dispersion for the flux phase at $x=0^+$ (solid line), 0.15 (dashed line), and 0.30 (dot-dashed line), and the paramagnetic phase at $x=0.45$ (dotted line).

displays a gap consistent with the small pseudogap, Fig. 7. However, this agreement breaks down at intermediate dopings. Figure 5 shows that the density wave gap decreases with decreasing x, while the experimental gap increases. Moreover, since the two pseudogaps have independent origins—a CDW or a flux phase—a theory involving uniform phases cannot explain their coexistence. In the following section, it will be shown that dynamic phase separation allows a smooth evolution between the two limits.

VI. CALCULATIONS FOR STRIPED PHASES

In the presence of phase separation, the dispersion will change. For a macroscopic phase separation, the photoemission would be a superposition of the two coexisting phases. However, in the present case, the phase separation is due to the holes only, so due to strong Coulomb effects (charging of the domains), the ensuing phase separation is on a nanoscopic scale only, which should lead to a more complex dispersion. There is evidence that in the cuprates, the phase separation is manifested in the form of alternating charge and magnetic stripes,[33,34] with a well defined periodicity that varies smoothly with doping. For any commensurate periodicity, the dispersion will have additional minigaps associated with the superlattice periodicity.[66] Since the stripes are generally dynamic, these superlattice gaps will probably be washed out.

A proper calculation of the self-consistent, dynamic stripe phases is beyond the scope of the current paper. Instead, I will suggest a number of plausible forms for the average dispersion, and show that it is possible to explain the observed photoemission data. There is considerable flexibility in the results, and it appears likely that different dispersions can be observed, depending on the spacing of the stripes, and on whether the stripes are effectively static or dynamic (i.e, on the time scale of the observational technique).

A. Large stripes

To simplify the problem, it is assumed that the fluctuations lead to a disorder in which any local region could have either of the two dispersions at random. The average dispersion can then be calculated by a coherent phase approximation calculation.[67,66] Repeating the calculation of Ref. 66, but assuming a random mix of only two-phases, with Green's functions G_1 and G_2 and probabilities p_1 and $p_2=1-p_1$, the average Green's function is (exactly) given by

$$G_0=p_1G_1+p_2G_2. \tag{13}$$

(Note that the assumption that the domains are large enough to have well defined G_1,G_2 is an implicit assumption of macroscopic phase separation.) Since the dispersion is given by real solutions of $G_0^{-1}=0$, the photoemission dispersion should simply be a weighted superposition of the dispersions of the two end phases, with $G_1^{-1}=0$ or $G_2^{-1}=0$. [The latter correspond to the eigenvalues of the Hamiltonian, Eq. (1), in the two coexisting phases.] A similar solution was found in Refs. 68,13.

Here, the distinction between the flux phase being at $x=0$ or 0^+ can be readily understood. At $x=0$, the Fermi level lies in the middle of the charge-transfer gap (taken to be half of the discontinuity in chemical potential in passing through $x=0$). Hence, the doping dependence predicted by Eq. (13) implies a gapped state at half filling, which persists in the doped material, with the appearance of midgap states in the doped material, with intensity increasing linearly with x. This is the form discussed in Refs. 68,13, and seems to provide a good description of photoemission experiments in a number of three-dimensional d-electron systems.[69] It would also be consistent with the photoemission data on underdoped YBCO,[63] although it is not clear why these data are inconsistent with the heat capacity results.[61]

However, this does not provide a good description of the photoemission data in Bi-2212, Fig. 7. A simple modification of the theory can significantly improve the agreement. If the phase separation starts not at $x=0$, but at a small positive doping $x_1=0^+$, then the doping dependence of the photoemission would be as follows. For doping between $x=0$ and x_1, there is no phase separation. The system remains in the flux phase, with the Fermi level again at midgap in undoped material, but shifting immediately to the top of the charge transfer band as soon as the first holes are doped in. This state is in good agreement with the experimental data on the most underdoped Bi-2212 samples, Fig. 7. With increased doping, the two-phase regime is reached. (Note that in this doped regime, the optical conductivity can still see a charge-transfer gap.[2])

The present model would predict a superposition of the two end phases, rather similar to Campuzano's interpretation of the data, but not consistent with the continuous evolution of the pseudogap suggested by the Stanford[50] and Loram[61,62] results. This lack of agreement is not surprising. Such a macroscopic phase separation would also predict a unique value of the superconducting transition temperature T_c (the flux phase at x_1 being nonsuperconducting). The experimental observation that T_c evolves smoothly with doping strongly suggests that the phase separation is on such a nanoscopic scale that T_c evolves with doping via a form of proximity

effect between the two phases. This same effect should explain the observed behavior of the pseudogap.

On a deeper level, the striped phases constitute a new thermodynamic state of matter, which can have a doping dependent T_c. A good analogy is provided by a superconductor in a magnetic field. In a type I superconductor, there is a macroscopic phase separation between domains wherein the magnetic field is nonzero, quenching the superconductivity, and superconducting domains with zero field. Increasing the field reduces the fraction of the material which is superconducting, but T_c does not change with field. In a type II superconductor, the field domains are shrunk down to nanoscopic size as magnetic vortices, producing a novel state of matter in which T_c is a continuously varying function of the field. In the following subsections, a model is provided for the pseudogap in the striped phases.

B. Small static stripes

If the stripe pattern is static and commensurate with the crystalline lattice, then the stripes will provide a superlattice to modify the dispersion of the separate phases. Since the resulting dispersion is profoundly modified, it would be appropriate to repeat the self-consistent calculations in the presence of the stripes. Without attempting this difficult procedure, however, a qualitative understanding of the results can be achieved by using the self-consistent band parameters calculated for the two phases in equilibrium, at $x=x_1>0$ and $x=x_c$. For definiteness, the end phases are assumed to be the flux phase at $x_1=0^+$ and the paramagnetic phase with $V_{\rm ep}=0.6$ eV, $x_c=0.288$. The fraction of charged stripes is then $\nu_c=x/x_c$.

Specifically, the stripes are assumed to be uniform along the y direction, and of periodicity $m+n$ Cu atoms along x, with m Cu atoms in the magnetic phase and n Cu's in the charged phase ($x=x_c$). For the cuprates, the x and y axes run parallel to the Cu-O-Cu bonds. All of the band parameters can be assigned values corresponding to either the flux phase at x_1 or the paramagnetic phase at x_c, except for the magnetic coupling of a Cu atom in the magnetic phase with a neighboring Cu in the charged phase. For these atoms, Δ_1 is taken as the average of the magnitudes of the Δ_1's in the two phases, with zero-phase factor. With these assumptions, the dispersion is a unique function of m and n. Figures 9 ($m=n=2$) and 10 ($m=2$, $n=6$) provide representative illustrations of the complicated dispersion to be expected. There are $2(m+n)$ subbands, with very small dispersion along the x direction, since $t\simeq 0$ in the flux phase. Note that, because of this small dispersion along X, the dispersion along $\Gamma\rightarrow Y$ is nearly the same as that along $X\rightarrow S$.

Once again, the results do not greatly resemble the photoemission data. Presumably, this is because the domains are fluctuating dynamically.[70] If photoemission from a static domain pattern could be observed, then the minigaps predicted here should be observed as long as the domains are nearly commensurate and disorder effects are small. In particular, the dispersion of Fig. 9 has a hole doping $x_c/2=0.144$, and should be similar to the $x=1/8$ phase of LSCO and $La_{2-x}Ba_xCuO_4$. [Note that the experiments of Tranquada *et al.*[33] determined the overall periodicity of the stripes, but only *assumed*, on analogy with the nickelates, that the charge stripes were one cell wide, corresponding to a hole doping $x=0.5$. An equally good case can be made[13] for the assumption that the charge stripes are two cells wide, with $x\simeq 0.25$; for instance, VHS nesting at $(\pi/a,\pi/a)$ is not well defined unless a stripe is at least two cells wide. A two-cell-wide charge stripe is consistent with the results of White and Scalapino.[71]]

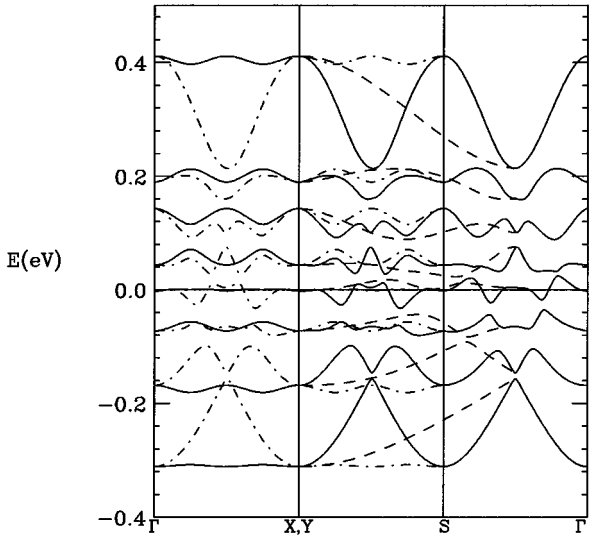

FIG. 9. Energy dispersion for a static striped phase, with $n=2$ charge layers and $m=2$ magnetic layers. Solid line (dot-dashed line): dispersion along $\Gamma\rightarrow X(Y)\rightarrow S$; dashed line: dispersion along $X\rightarrow S/2$.

C. Dynamic stripes

Notice that once nanoscopic stripes are formed, the averaging inherent in Eq. (13) is lost: no domain is large enough to have the dispersion characteristic of G_1. Now the band parameters have become local functions of space and, in dynamic stripes, of time as well. This can best be thought of as

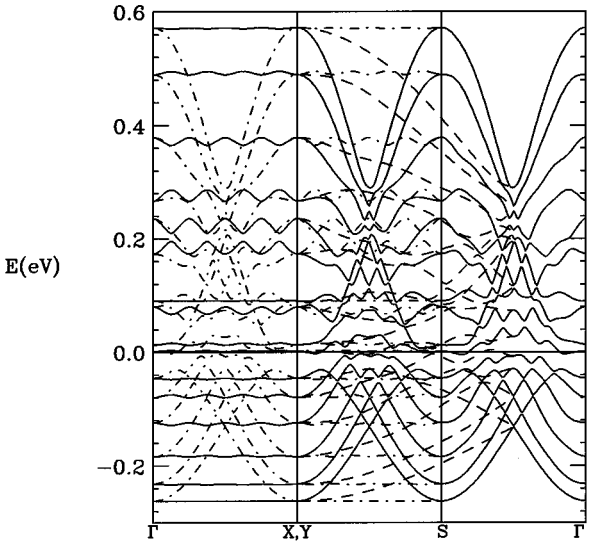

FIG. 10. Energy dispersion for a static striped phase, as for Fig. 9, but with $n=6$ charge layers and $m=2$ magnetic layers.

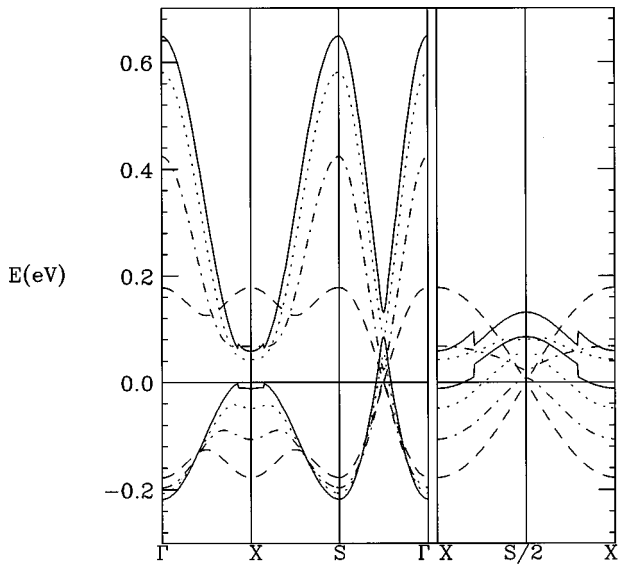

FIG. 11. Energy dispersion for the fluctuating stripe phase model, for $\nu_c=0$ (dashed line), 0.5 (dot-dashed line), 0.75 (dotted line), and 1 (solid line).

a generalization of the zero sound modes of a Landau Fermi-liquid–shape oscillations of the Fermi surface due to electron-electron interaction. I propose that in this state, when the stripe motion is rapid enough that only average properties are apparent, the appropriate procedure [replacing Eq. (13)] is to *average the band parameters themselves.*

This is done in Fig. 11, for several intermediate dopings. The resulting dispersions are in good agreement with the experimental data, Fig. 7. The photoemission studies find that at optimal doping, the Fermi level is close to an *extended* VHS, which evolves into a bifurcated VHS in underdoped Bi-2212 (for a bifurcated VHS, the dispersion has two minima offset from the X point along the Γ-X line of the Brillouin zone). These results are well reproduced in the present calculations.

Figure 12 shows the calculated DOS, illustrating the splitting of the VHS degeneracy. Note that in the unmodulated phase at $x=x_c=0.288$, the VHS is split, but there is no true gap [with $N(E)=0$]. This is because the δ_0 gap has a dispersion, so parts of the Fermi surface remain ungapped, at least in the absence of superconductivity. For lower doping,

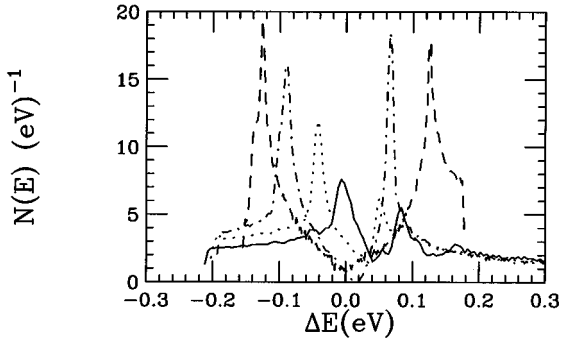

FIG. 12. Density of states vs energy $\Delta E=E-E_F$ for the fluctuating stripe phase model, for $\nu_c=0$ (dashed line), 0.5 (dot-dashed line), 0.75 (dotted line), and 1 (solid line).

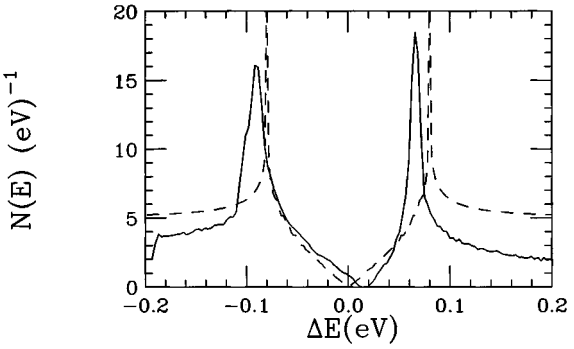

FIG. 13. Density of states vs energy $\Delta E=E-E_F$ for the fluctuating stripe phase model, for $\nu_c=0.5$ (solid line), compared to the calculated dos for a d-wave gap (dashed line).

the effective Fermi surface becomes closer to a square, and there is a gap over the full Fermi surface.

One must be careful about interpreting the DOS above the Fermi level in Fig. 12, because of the way the splitting into upper and lower Hubbard bands is accounted for in the slave-boson calculations. The figure illustrates the *spinon* DOS, while the particle DOS is given by a convolution of spinon and holon contributions. This is most easily illustrated at half filling: the convolution leaves the DOS below the Fermi level unchanged, while shifting the part above E_F across the charge-transfer gap.

Given the large splitting of the VHS degeneracy near the X point, one would expect a large interband absorption associated with inter-VHS scattering. If it is recalled that the experimental dispersion is about a factor of two larger than calculated (see Fig. 7), then this absorption could readily be identified with the well-known midinfrared absorption in the cuprates.[72] This feature displays a considerable shift as a function of hole doping, being centered at about 0.5 eV at very low dopings, while at optimal doping, the peak has moved to $\sim$0.1 eV. The present interpretation of the splitting would be consistent (at least near optimal doping) with the model of ''electronic polarons'' analogous to Zhang-Rice singlets.[73] In the low doping regime, there may be additional absorption peaks associated with an isolated charge stripe, as suggested by the large number of very flat bands along $\Gamma\rightarrow X$ in Figs. 9,10.

The opening of the pseudogap with underdoping found in Fig. 12 is in good qualitative agreement with the heat capacity measurements of Loram *et al.*[61,62] They have fit the DOS line shape to a d-wave gap, and Fig. 13 shows that the DOS calculated for $\nu_c=0.5$ does indeed bear a strong resemblance to a d-wave gap (dashed line).

A closer comparison of the data, Fig. 7, and the theory, Fig. 11, reveals excellent agreement near Γ (e.g., along $\Gamma\rightarrow X$), but an absence of the experimental points near $S=(\pi,\pi)$ (e.g., along $X\rightarrow S$). This is the ''ghost'' part of the dispersion, due to the presence of a superlattice associated with CDW or magnetic order. The absence of this ghost dispersion near optimal doping is additional evidence for the absence of long-range CDW order, albeit rather weak evidence. Note that the ghost dispersion is also greatly smeared out in the limiting case of SCOC (squares in Fig. 7), which has well defined magnetic order. While the photoemission data were taken at a temperature (350 K) above the Néel temperature (265 K), the magnetic correlation length was still much larger than the effective size sampled by neutrons,

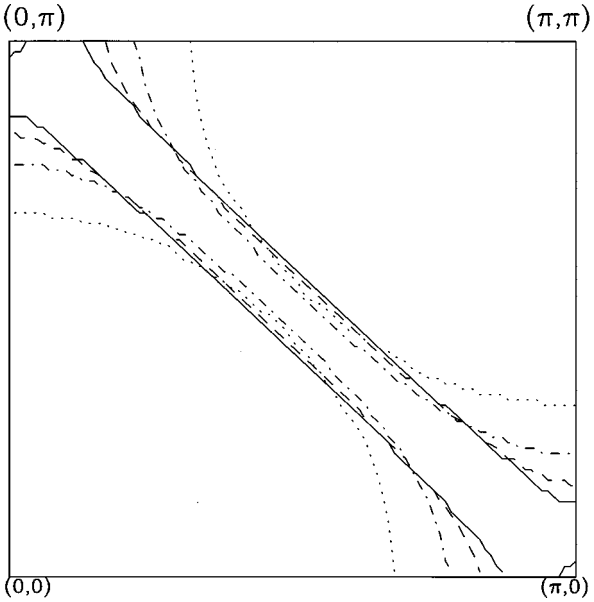

FIG. 14. Fermi surfaces for the fluctuating stripe phase model, for $\nu_c=1.0$ (dotted line), 0.625 (dot-dashed line), 0.5625 (dashed line), and 0.5486 (solid line).

so local antiferromagnetic order was present.[51] Moreover, Bi-2212 has a well-defined structural orthorhombic superlattice, but the ghost dispersion remains extremely weak.[74] The evolution of the Fermi surface with doping shows a clear crossover from a large Fermi surface, Fig. 14, to a small Fermi surface, Fig. 15. Once again, the shapes of the Fermi surfaces are in good agreement with photoemission, except in the ghost part of the dispersion.

Note that while the theoretical data in Figs. 1–7 are based on the self-consistent slave-boson calculations of the flux and paramagnetic phases or on the result of a more exact calculation[43,45] (the point marked $\times$ in Fig. 1), the results of this section, Figs. 11–15, require one additional assumption. This is the assumption that, in the presence of a dynamic stripe phase, the proper average over these stripes is given by the weighted average of the band parameters of the two coexisting phases. The present results are consistent with the findings of Salkola *et al.*[70] They calculated the photoemission spectra of a phenomenological stripe phase Hamiltonian, and found that (1) for a regular stripe array, the dispersion is dominated by minigaps, and bears little resemblance to experiment; and (2) for a quenched random distribution of stripes (taken as representative of dynamically fluctuating stripes) there is a single average photoemission spectrum, which resembles the experimental observations.

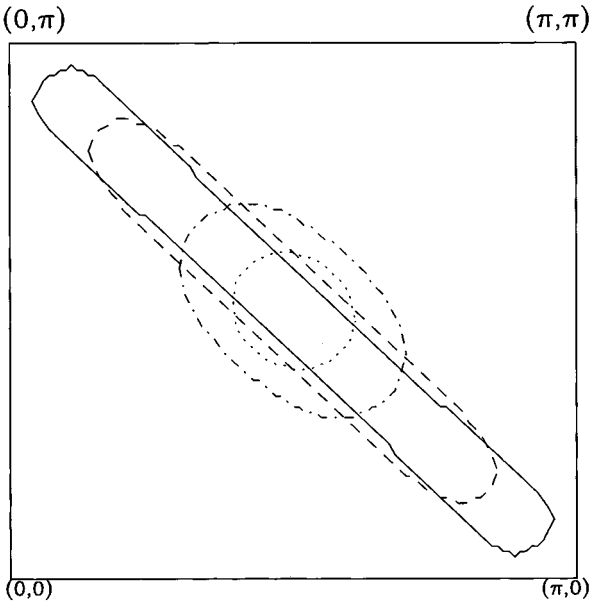

FIG. 15. Fermi surfaces for the fluctuating stripe phase model, for $\nu_c=0.125$ (dotted line), 0.25 (dot-dashed line), 0.5 (dashed line), and 0.5469 (solid line).

D. Relation to other phonon calculations

A number of other groups[75–82] have also explored the possibility of electron-phonon coupling to the breathing modes in the cuprates. The coupling is generally found to be strong, capable of generating CDW or striped phase instabilities. The present calculations are particularly close to the inhomogeneous Hartree-Fock calculations of Yonemitsu *et al.*,[76] which find a nanoscale phase separation between magnetic insulating and charged polaronic domains, rather similar to Goodenough's polaron bag model.[83] The slave-boson calculations of den Hertog and Das[82] should also be similar, but they find no evidence of VHS nesting. Indeed, the doping dependence of the CDW phase is completely featureless, and the CDW actually raises the energy of the system. These results are more similar to what I found for the *electron* doped regime; the reason for these differences is not understood at present.

Whereas the breathing mode is at $(\pi/a,\pi/a)$, experiment finds the strong phonon softening associated with modes near $(\pi/a,0)$.[84,85] A possible resolution of this problem is that the observed mode softening may be caused by the striped phases themselves,[86] which are aligned along $(\pi/a,0)$ in LSCO.

VII. DISCUSSION

The above calculations have provided a plausible explanation for the opening of a double pseudogap in underdoped Bi-2212, while providing a sounder underpinning for the earlier one-band calculations of Ref. 25. The present results are in excellent agreement with these earlier calculations, which can therefore be used to supplement the present $T=0$ calculations. Here, the detailed correspondence between experiment and theory will be briefly summarized, including calculations of superconducting properties and temperature dependences from the one-band model.

First and foremost, it should be noted that Fig. 12 is a very clear demonstration that the physics of the underdoped cuprates is dominated by VHS nesting, with the splitting of the DOS peak increasing smoothly with increased underdoping. Second, the model is not merely consistent with the underlying presence of striped phases (or similar manifestations of nanoscale phase separation), it *requires* them to reproduce the smooth doping dependence of the pseudogap magnitude. Third, it correctly reproduces the characteristic double gap structure which has been such a puzzling feature of the photoemission experiments: the large splitting of the

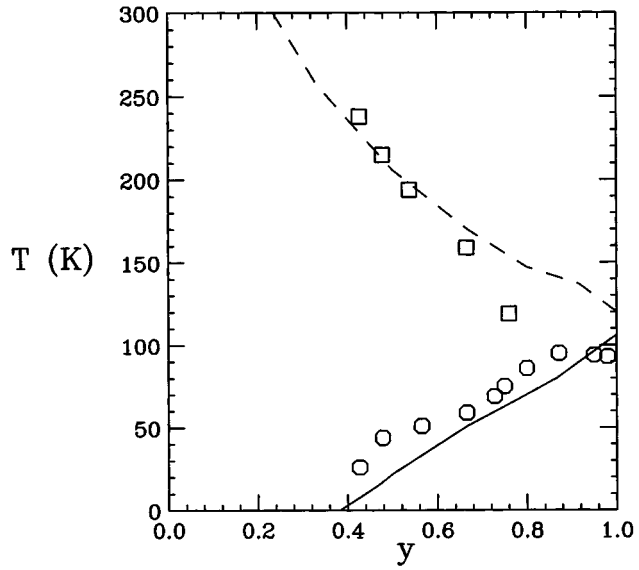

FIG. 16. Phase diagram of the pseudogap (dashed line) and superconducting (solid line) phases, based on the one-band model, and compared to the experimental data of Loram *et al.* (Ref. 87) for $YBa_2Cu_3O_{6+y}$.

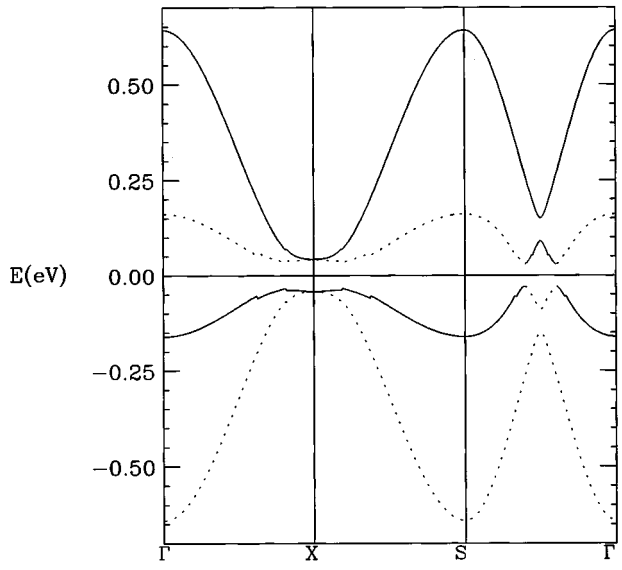

FIG. 17. Energy dispersion in the one-band model, in the presence of superconductivity. Dotted line is the hole-like part of dispersion (electron-like part reflected around Fermi level). Only the electronlike part (solid lines) will be visible in, e.g., a photoemission experiment. To stress the role of the superconducting gap, the smaller CDW gap, δ_1, has been set equal to zero.

VHS degeneracy, associated with δ_0, and the smaller pulling back of DOS from the Fermi level, associated with δ_1. Since both are aspects of a single transition, both disappear at the same pseudogap transition temperature, as found experimentally.

Figure 16 (Ref. 26) shows that the model reproduces the experimentally observed[87] pseudogap phase diagram, including a doping dependent superconducting T_c. The competition between pseudogap and superconductivity displayed in Fig. 16 can be understood in terms of the evolution of the shape of the Fermi surface with doping. The VHS is pinned by correlation and phase separation effects near the Fermi surface; this pinning means that the shape of the Fermi surface must evolve with doping, being square at half filling, and curved in such a way as to accomodate more holes as doping increases. Since the pseudogap is associated with nesting, it dominates near half filling, when the nesting is perfect. Away from half filling, the nesting is worse, so the pseudogap and pseudogap transition temperature both rapidly decrease with doping. Superconductivity requires a large DOS, but is insensitive to nesting; moreover, it can arise on those sections of Fermi surface which survive the imperfect nesting. For both of these reasons, the superconducting transition temperature grows with increasing doping, until it is comparable to the density-wave transition.

Within the model, the pseudogap arises from a structural or magnetic instability—actually, there is a crossover between the two effects with increased underdoping. Neither has any direct relation with superconductivity, except that they compete with it for the large DOS associated with the VHS. Superconductivity first arises in the model from the leftover DOS associated with parts of the Fermi surface away from the VHS. This is illustrated in the one-band model calculation of Fig. 17, which shows how the electronic dispersion, in the presence of a density-wave gap, is modified by the appearence of a superconducting gap. (In the figure, an *s*-wave gap is assumed, consistent with the earlier calculation.[25] Just how these features are modified by a more realistic *d*-wave gap will be explored in a future publication.) In this figure, the holelike parts of the Fermi surface (dotted lines) are ghosts, with the intensity suppressed by coherence factors, and will not be observed by photoemission. The solid lines in this figure should be compared to the dotted lines in Fig. 11. The main difference is the superconducting gap away from the VHS—mainly near the hole pockets at $S/2$, although there is a weak superconducting contribution to the gap at the VHS. Thus, unlike Fig. 12, in the presence of a superconducting gap, the DOS will vanish at the Fermi level (except at isolated points for a *d*-wave gap).

Hence, in the present model, the smaller photoemission gap near the Fermi level is a composite object, due in part to superconductivity but also in part to the density-wave gap. This explains why a gap persists near $(\pi,0)$ in the pseudogap regime above the superconducting T_c. However, at T_c there should be subtle changes in the form of the gap—in particular, above T_c, the density-wave gaps should vanish not just at $S/2$ (for a *d*-wave gap), but in a finite portion of the Brillouin zone near $S/2$. The present model would predict a scaling of the superconducting part of the gap with T_c, and hence with ν_c.[25] Evidence for such a gap feature is found in neutron scattering measurements of the magnetic susceptibility near $S=(\pi,\pi)$, which see a spin gap followed by a resonance peak, both of which features scale with T_c.[88] Such a spin gap follows from BCS theory. To be consistent with Fig. 17, the susceptibility must be associated with scattering between sections of Fermi surface near $S/2$ which are not gapped by the density-wave order.

Thus, the present model has two density-wave-like gaps, a large one associated with VHS splitting and a smaller tied to the Fermi surface, which approximately scale together and are both largest near half filling, and a superconducting gap which has the opposite doping dependence. The overall simi-

larity to the phase diagram deduced by Batlogg and Emery[89] should be noted.

Within the present model, the issue of *overdoping* can be briefly addressed. From the free energy curves of Fig. 2, it appears that the system will continue to evolve in a uniform paramagnetic phase for doping beyond the phase separated regime. However, the free energy has a local minimum near optimal doping, which is likely to be enhanced by the difficulty of adding additional holes to the CuO_2 planes. Hence, there may well be another phase with lower free energy, probably associated with doping holes off of the planes (perhaps onto the apical O's and Cu-d_{z^2}'s) in this doping range. The crossover from the optimally doped phase to this overdoped phase will probably again involve a phase separation. Experimental evidence for a second phase separation in the overdoped regime is summarized in Ref. 13, Section 11.6. This does not preclude the possibility that there is a small but finite range of doping near the optimal in which a single phase solution is stable. Whereas in YBCO the pseudogap and superconducting transition temperatures coincide at optimal doping, in LSCO the pseudogap temperature is considerably higher than T_c, even at optimal doping.[13] Interestingly, heat capacity measurements in LSCO (Ref. 61) find that the gap closes to a single VHS peak at the Fermi level (see Fig. 21 of Ref. 13) in the overdoped range, $x=0.27$. For larger overdopings, this peak remains at the Fermi level, but decreases in intensity (as might be expected in the presence of a phase separation). This suggests an even stronger pinning of the Fermi level to the VHS than expected theoretically. Note from Fig. 2 that in the overdoped regime, the CDW undergoes a quantum phase transition, $T_{\mathrm{CDW}}\rightarrow 0$. The possible role of such a QCP on superconductivity has been discussed recently.[90] However, this could be obscured by a second phase separation in the overdoped regime.

There have been a number of alternative interpretations of the pseudogap. The strictly magnetic models[91] have difficulty explaining why a gap is also seen in the charge spectrum, including photoemission and heat capacity. Other models suggest that it is associated with local pair formation, as a precursor effect to superconductivity.[92] However, in overdoped materials, the pseudogap transition lies at a lower temperature than the superconducting transition.[93] Moreover, these models do not explain the frequent association of the pseudogap with structural anomalies, Ref. 13, Sections 9.1,2.

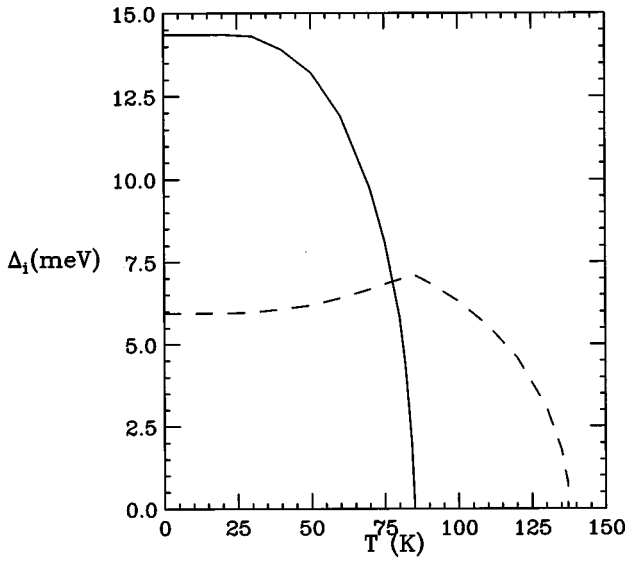

FIG. 18. Temperature dependences of the pseudogap (dashed line) and the superconducting gap (solid line) in the one-band model.

Perhaps the clearest example is in $YBa_2Cu_4O_8$. Even when stoichiometric, this material is underdoped, behaving in many ways like $YBa_2Cu_3O_{6.6}$, with a pseudogap onset near 150 K. When some of the Y is replaced by Ca, a transition to a long-range structually ordered phase is found at nearly the same transition temperature.[94] Moreover, the theory predicts that, in the doping range where both phases coexist, the onset of superconductivity leads to a softening of the pseudogap, Fig. 18. This can explain a number of observations of lattice anomalies at T_c, Ref. 13, Section 9.3.

While the present model provides an impressive picture for pseudogap formation in the presence of dynamic stripes, it must be recalled that a number of intermediate steps need to be filled in. These include (1) self-consistent calculation of the band parameters in a static striped phase; and (2) incorporation of dynamical fluctuations into the calculation. In addition, (3) a more detailed analysis of just which phonon modes are coupled is necessary, to see how both the smaller DW gap and the superconducting gap can be *d* wave. Despite these limitations, it is clear that the present calculations have the ability to explain both the stripes and the pseudogap within a common theoretical framework.

[1] P. Coleman, Phys. Rev. B **28**, 5255 (1983); N. Read and D. Newns, Solid State Commun. **52**, 933 (1984); A. Auerbach and K. Levin, Phys. Rev. Lett. **57**, 877 (1987).

[2] G. Kotliar, P.A. Lee, and N. Read, Physica C **153-155**, 538 (1988).

[3] C.A.R. Sa de Melo and S. Doniach, Phys. Rev. B **41**, 6633 (1990).

[4] R.S. Markiewicz, J. Phys.: Condens. Matter **2**, 665 (1990).

[5] M. Grilli, B.G. Kotliar, and A.J. Millis, Phys. Rev. B **42**, 329 (1990).

[6] D. M. Newns, P.C. Pattnaik, and C.C. Tsuei, Phys. Rev. B **43**, 3075 (1991).

[7] E. Dagotto, A. Nazarenko, and M. Boninsegni, Phys. Rev. Lett. **73**, 728 (1994); N. Bulut, D.J. Scalapino, and S.R. White, *ibid.* **73**, 748 (1994); Phys. Rev. B **50**, 7215 (1994).

[8] C. Castellani, G. Kotliar, R. Raimondi, M. Grilli, Z. Wang, and M. Rozenberg, Phys. Rev. Lett. **69**, 2009 (1992).

[9] R.S. Markiewicz, Physica C **228**, 227 (1994).

[10] H. Endres, W. Hanke, H.G. Evertz, and F.F. Assaad, Phys. Rev. Lett. **78**, 160 (1997).

[11] G. Dopf, A. Muramatsu, and W. Hanke, Phys. Rev. B **41**, 9264 (1990).

[12] R.T. Scalettar, D.J. Scalapino, R.L. Sugar, and S.R. White, Phys. Rev. B **44**, 770 (1991).

[13] R.S. Markiewicz, J. Phys. Chem. Solids. **58**, 1179 (1997).

[14] P.H. Dickinson and S. Doniach, Phys. Rev. B **47**, 11 447 (1993).

[15] S. Caprara and M. Grilli, Phys. Rev. B **49**, 6971 (1994).
[16] S. Caprara, C. DiCastro, and M. Grilli, Phys. Rev. B **51**, 9286 (1995).
[17] R.S. Markiewicz (unpublished); and presented at the *First International Conference on Stripes, Lattice, Instabilities, and High T_c Superconductivity, Rome, Dec. 8–12, 1996* [Ref. 29(c)].
[18] Q. Si and K. Levin, Phys. Rev. B **44**, 4727 (1991).
[19] Q. Si and G. Kotliar, Phys. Rev. B **48**, 13 881 (1993).
[20] P. Monthoux and D. Pines, Phys. Rev. B **47**, 6069 (1993).
[21] K. Dichtel, J. Fritzenkötter, and J. Carstensen, *Phase Separation in Cuprate Superconductors* [Ref. 29(b)], p. 365.
[22] D.J. Golosov, M.L. Horbach, and A.E. Ruckenstein, J. Supercond. **8**, 659 (1995).
[23] J. González, F. Guinea, and M.A.H. Vozmediano, Europhys. Lett. **34**, 711 (1996), and (unpublished).
[24] P. Majumdar and H.R. Krishnamurthy (unpublished).
[25] R.S. Markiewicz, Physica C **193**, 323 (1992).
[26] R.S. Markiewicz, Phys. Rev. Lett. **73**, 1310 (1994).
[27] G. Kotliar, Phys. Rev. B **37**, 3664 (1988); I. Affleck and J.B. Marston, *ibid.* **37**, 3774 (1988).
[28] C.A. Balseiro and L.M. Falicov, Phys. Rev. B **20**, 4457 (1979).
[29] (a) *Phase Separation in Cuprate Superconductors*, edited by K.A. Müller and G. Benedek (World, Singapore, 1992); (b) *Phase Separation in Cuprate Superconductors*, edited by E. Sigmund and K.A. Müller (Springer, Berlin, 1994); (c) *First International Conference on Stripes, Lattice Instabilities, and High T_c Superconductivity, Rome, Dec. 8-12, 1996* [J. Supercond. (to be published)].
[30] V.J. Emery and S.A. Kivelson, Physica C **209**, 597 (1993).
[31] R.S. Markiewicz, Int. J. Mod. Phys. B **5**, 2037 (1991).
[32] J.D. Jorgensen, B. Dabrowski, S. Pei, D.G. Hinks, L. Soderholm, B. Morosin, J.E. Schirber, E.L. Venturini, and D.S. Ginley, Phys. Rev. B **38**, 11 337 (1988): M.S. Hundley, J.D. Thompson, S-W. Cheong, Z. Fisk, and J.E. Schirber, *ibid.* **41**, 4062 (1990); P.C. Hammel, A.P. Reyes, Z. Fisk, M. Takigawa, J.D. Thompson, R.H. Heffner, S-W. Cheong, and J.E. Schirber, *ibid.* **42**, 6781 (1990).
[33] J.M. Tranquada, B.J. Sternlieb, J.D. Axe, Y. Nakamura, and S. Uchida, Nature (London) **375**, 561 (1995).
[34] J.M. Tranquada, J.D. Axe, N. Ichikawa, A.R. Moodenbaugh, Y. Nakamura, and S. Uchida, Phys. Rev. Lett. **78**, 338 (1997).
[35] P.B. Visscher, Phys. Rev. B **10**, 943 (1974).
[36] E.L. Nagaev, *Physics of Magnetic Semiconductors* (Moscow, Mir, 1983).
[37] V. Hizhnyakov and E. Sigmund, Physica C **156**, 655 (1988).
[38] V.J. Emery, S.A. Kivelson, and H.Q. Lin, Phys. Rev. Lett. **64**, 475 (1990).
[39] C. Au, B.H. Zhao, and H.T. Nieh, Phys. Rev. Lett. (to be published); G. Su, Phys. Rev. B **54**, 8281 (1996).
[40] E. Dagotto, Rev. Mod. Phys. **66**, 763 (1994).
[41] R. Raimondi, C. Castellani, M. Grilli, Y. Bang, and G. Kotliar, Phys. Rev. B **47**, 3331 (1993).
[42] E. Ercolessi, P. Pieri, and M. Roncaglia (unpublished).
[43] C.S. Hellberg and E. Manousakis, Phys. Rev. Lett. **78**, 4609 (1997).
[44] F. Basco, H. Kohno, H. Fukuyama, and G. Baskaran, J. Phys. Soc. Jpn. **65**, 687 (1996).
[45] E. Manousakis, Rev. Mod. Phys. **63**, 1 (1991).
[46] F.C. Zhang and P. Prelovsek, Phys. Rev. B **37**, 1569 (1988).
[47] S. Tang and J.E. Hirsch, Phys. Rev. B **37**, 9546 (1988).
[48] R.S. Markiewicz, Physica C **255**, 211 (1995).
[49] A.A. Abrikosov, J.C. Campuzano, and K. Gofron, Physica C **214**, 73 (1993): K. Gofron, J.C. Campuzano, A.A. Abrikosov, M. Lindroos, A. Bansil, H. Ding, D. Koelling, and B. Dabrowski, Phys. Rev. Lett. **73**, 3302 (1994).
[50] D.S. Marshall, D.S. Dessau, A.G. Loeser, C.-H. Park, A.Y. Matsuura, J.N. Eckstein, I. Bozovic, P. Fournier, A. Kapitulnik, W.E. Spicer, and Z.-X. Shen, Phys. Rev. Lett. **76**, 4841 (1996).
[51] B.O. Wells, Z.X. Shen, A. Matsuura, D.M. King, M.A. Kastner, M. Greven, and R.J. Birgeneau, Phys. Rev. Lett. **74**, 964 (1995).
[52] E. Dagotto, A. Nazarenko, and A. Moreo, Phys. Rev. Lett. **74**, 310 (1995).
[53] A. Nazarenko, K.J.E. Vos, S. Haas, E. Dagotto, and R.J. Gooding, J. Supercond. **8**, 671 (1995).
[54] R.B. Laughlin, J. Phys. Chem. Solids **56**, 1627 (1995).
[55] X.-G. Wen and P.A. Lee, Phys. Rev. Lett. **76**, 503 (1996).
[56] U. Trapper, D. Ihle, and H. Fehske, Phys. Rev. B **52**, 11 553 (1995).
[57] Y.R. Wang, Phys. Rev. B **43**, 3786 (1991); **46**, 151 (1992).
[58] A.G. Loeser, D.S. Dessau, and Z.-X. Shen, Physica C **263**, 208 (1996); A.G. Loeser, Z.-X. Shen, D.S. Dessau, D.S. Marshall, C.H. Park, P. Fournier, and A. Kapitulnik, Science **273**, 325 (1996).
[59] H. Ding, T. Yokoya, J.C. Campuzano, T. Takahashi, M. Randeria, M.R. Norman, T. Mochiku, K. Kadowaki, and J. Giapintzakis, Nature (London) **382**, 51 (1996).
[60] J.C. Campuzano, presented at the *First International Conference on Stripes, Lattice, Instabilities, and High-T_c Superconductivity, Rome, Dec. 8–12, 1996*, [Ref. 29(c)].
[61] J.W. Loram, J.R. Cooper, K.A. Mirza, N. Athanassopoulou, and W.Y. Liang (unpublished).
[62] J.W. Loram, K.A. Mirza, J.R. Cooper, N. Athanassopoulou, and W.Y. Liang, in *Proceedings of the 10th Anniversary HTS Workshop on Physics, Materials, and Applications*, edited by B. Batlogg, C. W. Chu, W. K. Chu, D. U. Gubser, and K. A. Müller (World Scientific, Singapore, 1996), p. 341.
[63] R. Liu, B.W. Veal, A.P. Paulikas, J.W. Downey, H. Shi, C.G. Olson, C. Gu, A.J. Arko, and J.J. Joyce, Phys. Rev. B **45**, 5614 (1992); R. Liu, B.W. Veal, A.P. Paulikas, J.W. Downey, P.J. Kostic, S. Fleshler, U. Welp, C.G. Olson, X. Wu, A.J. Arko, and J.J. Joyce, *ibid.* **46**, 11 056 (1992).
[64] R. Liu, B.W. Veal, C. Gu, A.P. Paulikas, P. Kostic, and C.G. Olson, Phys. Rev. B **52**, 553 (1995).
[65] R. Preuss, W. Hanke, C. Gröber, and H.G. Everts, Phys. Rev. Lett. **79**, 1122 (1997).
[66] R.S. Markiewicz, Physica C **207**, 281 (1993).
[67] R.J. Elliott, J.A. Krumhansl, and P.L. Leath, Rev. Mod. Phys. **46**, 465 (1974).
[68] H. Kajueter, G. Kotliar, and G. Moeller, Phys. Rev. B **53**, 16 214 (1996); D.D. Sarma, S.R. Barman, H. Kajueter, and G. Kotliar, Europhys. Lett. **36**, 307 (1996).
[69] A. Fujimori, I. Hase, H. Namatame, Y. Fujishima, Y. Tokura, H. Eisaki, S. Uchida, K. Takegahara, and F.M.F. deGroot, Phys. Rev. Lett. **69**, 1796 (1992); A. Fujimori, I. Hase, Y. Tokura, M. Abbate, F.M.F. deGroot, J.C. Fuggle, H. Eisaki, and S. Uchida, Physica B **186-188**, 981 (1993); I.H. Inoue, I. Hase, Y. Aiura, A. Fujimori, Y. Haruyama, T. Maruyama, and Y. Nishihara, Phys. Rev. Lett. **74**, 2539 (1995).
[70] M.I. Salkola, V.J. Emery, and S.A. Kivelson, Phys. Rev. Lett. **77**, 155 (1996).
[71] S.R. White and D.J. Scalapino, Phys. Rev. B **55**, 6504 (1997).
[72] D.B. Tanner and T. Timusk, in *Physical Properties of High Tem-*

perature Superconductors III, edited by D.M. Ginsberg (World Scientific, Singapore, 1992), p. 363.

[73] J. Lorenzana and L. Yu, Phys. Rev. Lett. **70**, 861 (1993); J. Lorenzana, Physica B **206-207**, 675 (1995).

[74] P. Aebi, J. Osterwalder, P. Schwaller, L. Schlapbach, M. Shimoda, T. Mochiku, and K. Kadowaki, Phys. Rev. Lett. **72**, 2757 (1994).

[75] H.-B. Schüttler, J. Zhong, and A.J. Fedro, in *Electronic Properties and Mechanisms of High T_c Superconductors*, edited by T. Oguchi, K. Kadowaki, and T. Sasaki (Elsevier, Amsterdam, 1992), p. 295.

[76] K. Yonemitsu, A.R. Bishop, and J. Lorenzana, Phys. Rev. Lett. **69**, 965 (1992); Phys. Rev. B **47**, 8065 (1993); **47**, 12 059 (1993).

[77] H. Fehske, M. Deeg, and H. Büttner, Phys. Rev. B **46**, 3713 (1992): M. Deeg, H. Fehske, and H. Büttner, Z. Phys. B **88**, 283 (1992); H. Fehske, H. Röder, G. Wellein, and A. Mistriotis, Phys. Rev. B **51**, 16 582 (1995).

[78] A. Dobry, A. Greco, S. Koval, and J. Riera, Phys. Rev. B **52**, 13 722 (1995).

[79] D. Poilblanc, T. Sakai, D.J. Scalapino, and W. Hanke, Europhys. Lett. **34**, 367 (1996).

[80] R. Fehrenbacher, Phys. Rev. Lett. **77**, 2288 (1996).

[81] F. Becca, M. Tarquini, M. Grilli, and C. Di Castro, Phys. Rev. B **54**, 12 443 (1996); M. Capone, M. Grilli, and W. Stephan (unpublished).

[82] B.C. den Hertog and M.P. Das, Phys. Rev. B **54**, 6693 (1996).

[83] J.B. Goodenough and J.-S. Zhou, Phys. Rev. B **42**, 4276 (1990).

[84] L. Pintschovius and W. Reichardt, in *Physical Properties of High Temperature Superconductors, IV*, edited by D.M. Ginsberg (World Scientific, Singapore, 1994), p. 295.

[85] W. Reichardt, L. Pintschovius, N. Pyka, P. Schweiss, A. Erb, P. Bourges, G. Collin, J. Rossat-Mignod, I.Y. Henry, A.S. Ivanov, N.L. Mitrofanov, and A.Yu. Rumiantsev, J. Supercond. **7**, 399 (1994).

[86] R.J. McQueeney, T. Egami, G. Shirane, and Y. Endoh, Phys. Rev. B **54**, 9689 (1996).

[87] J.W. Loram, K.A. Mirza, J.R. Cooper, and W.Y. Liang, Phys. Rev. Lett. **71**, 1740 (1993).

[88] P. Dai, M. Yethiraj, H.A. Mook, T.B. Lindemer, and F. Doğan, Phys. Rev. Lett. **77**, 5425 (1996); H.F. Fong, B. Keimer, D.L. Milius, and I.A. Aksay, *ibid.* **78**, 713 (1977).

[89] B. Batlogg and V.J. Emery, Nature (London) **382**, 20 (1996).

[90] A. Perali, C. Castellani, C. Di Castro, and M. Grilli, Phys. Rev. B **54**, 16 216 (1996).

[91] Y. Suzumura, Y. Hasegawa, and H. Fukuyama, J. Phys. Soc. Jpn. **57**, 401 (1988); N. Nagaosa and P.A. Lee, Phys. Rev. B **45**, 966 (1992); M.U. Ubbens and P.A. Lee, *ibid.* **49**, 6853 (1994).

[92] C.A.R. Sa de Melo, *et al.*, Phys. Rev. Lett. **71**, 3202 (1993); V.J. Emery and S.A. Kivelson, Nature (London) **274**, 434 (1995); J. Maly, K. Levin, and D.Z. Liu, Phys. Rev. B **54**, 15 657 (1996).

[93] J.L. Tallon, J.R. Cooper, P.S.I.P.N. de Silva, G.V.M. Williams, and J.W. Loram, Phys. Rev. Lett. **75**, 4114 (1995): P.J. White, Z.-X. Shen, C. Kim, J.M. Harris, A.G. Loeser, P. Fournier, and A. Kapitulnik, Phys. Rev. B **54**, 15 669 (1996).

[94] W. Ting, O.-M. Nes, T. Suzuki, M.G. Karkut, K. Fossheim, Y. Yaegashi, H. Yamauchi, and S. Tanaka, Phys. Rev. B **48**, 607 (1993); W. Ting and K. Fossheim, J. Alloys Compd. **211-212**, 260 (1994).